World Journal of Biology Pharmacy and Health Sciences, 2020, 03(01), 038–053

World Journal of Biology Pharmacy and Health Sciences

e-ISSN: 2582-5542, Cross Ref DOI: 10.30574/wjbphs

Journal homepage: http://www.wjbphs.com

(RESEARCH ARTICLE)

QSAR rationales for the PPARα/γ agonistic activity of 4,4-Dimethyl-1,2,3,4-tetrahydroquinoline derivatives

Parihar Raghuraj and Sharma Brij Kishore*

Department of Chemistry, Government College, Bundi-323 001 (Rajasthan), India.

Publication history: Received on 30 June 2020; revised on 16 July 2020; accepted on 18 July 2020

Article DOI: https://doi.org/10.30574/wjbphs.2020.3.1.0044

Abstract

The PPARγ binding affinity and transactivation profiles for hPPARα and hPPARγ of tetrahydroquinoline derivatives have been quantitatively analyzed in terms of topological 0D-, 1D- and 2D-descriptors based on molecular graph theory. Statistically sound models have been obtained between the biological actions and various DRAGON descriptors through combinatorial protocol-multiple linear regression (CP-MLR) computational procedure. Amongst the large number of such derived models, the most significant ones have only been discussed to draw meaningful conclusions. From the statistically significant models, it appeared that the mode of actions of titled compounds were different for hPPARα and hPPARγ transactivation profiles and PPARγ binding affinity. Applicability domain analysis carried out for PPARγ binding affinity revealed that the suggested model matches the high quality parameters with good fitting power and the capability of assessing external data and all of the compounds was within the applicability domain of the proposed model and were evaluated correctly.

Keywords: QSAR; PPARγ binding affinity; hPPARα and hPPARγ transactivation activity; Combinatorial protocol in multiple linear regression (CP-MLR) analysis; Dragon descriptors; 4,4-Dimethyl-1,2,3,4-tetrahydroquinolines.

1. Introduction

A complex metabolic disease, Type-2 diabetes (T2D), come with a defect in pancreaticβ-cell and is characterized by resistance of insulin in the liver and peripheral tissues [1]. T2D, due to lack of physical activity and excessive food intake, is presumed to attain epidemic proportions [2]. The treatment of T2D is currently aimed at to improve insulin secretion by reducing hyperglycemia or to reduce the insulin resistance of peripheral tissues. Most of such types of commonly used therapies were developed without considering therapeutic target. Therefore attempts were made to identify more suitable therapeutic strategies with better insight of the disease's pathogenesis [3]. Peroxisomes proliferators activated receptors (PPARs), belonging to the family of nuclear receptors, are ligand-activated transcription factors [4]. Three subtypes namely PPARα, PPARγ and PPARβ/(δ) have been identified after the discovery in 1990 by Issemen and Green [5]. These receptors are extensively involved in glucose and lipid homeostasis [6-8]. A number of agonists in this class have progressed to the clinical phase and marketed as anti-diabetic drugs [9,10].The hypolipidemic fibrates and glitazones class of insulin sensitizers, full-agonists of PPARα [4] and PPARγ [11,12], respectively, has motivated pharmaceutical companies to focus on developing more potent and dual acting agonists belonging to these two subtypes. In the treatment of dyslipidemic T2D dual-acting PPARα/γ agonists such as Tesaglitazar and Muraglitazar have been observed as a very attractive option [6,10, 13-18]. These compounds may also circumvent or reduce the main side effects such as weight gain or edema induced by the full PPARγ agonists like TZDs [19]. The ligand–protein interactions of a typical PPAR agonists revealed that the acidic head group of ligand, known as carboxylic acid, is involved in up to four hydrogen bounds with the receptor which is crucial part for activation of PPAR. The central aromatic moiety is located in a hydrophobic pocket while the cyclic tail tolerates more polar substituents [20]. Based on the typical topology of synthetic PPAR agonists 4,4-dimethyl-1,2,3,4-tetrahydroquinoline has been considered as novel cyclic tail to design novel PPARγ selective agonists and/or dual PPARα/γ agonists [21]. A new series of 4,4-

* Corresponding author: Sharma Brij Kishore

dimethyl-1,2,3,4-tetrahydroquinoline-based compounds as effective PPARγ selective agonists and dual-acting agonists of PPARα and PPARγ has been reported [22,23]. The aim of present communication is to establish the quantitative relationships between the reported activities and molecular descriptors unfolding the substitutional changes in titled compounds.

2. Material and methods

2.1. Biological actions and theoretical molecular descriptors

The reported eighteen tetrahydroquinoline derivatives are considered as the data set for this study [22,23]. The structures of these analogues are given in Table 1.

Table 1 Structures[a] of tetrahydroquinoline derivatives

Cpd.	Structure	Cpd.	Structure
1[b]	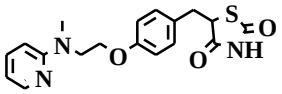	10	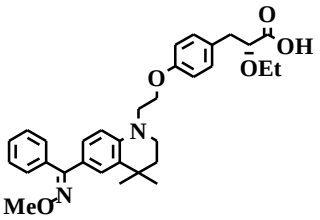
2[c]	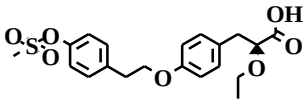	11	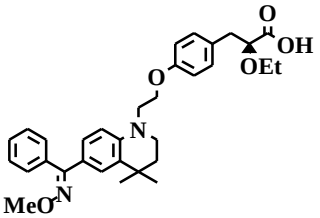
3	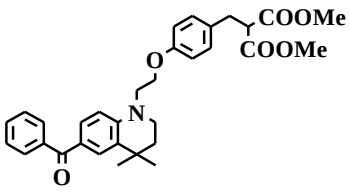	12	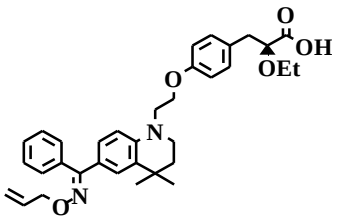
4	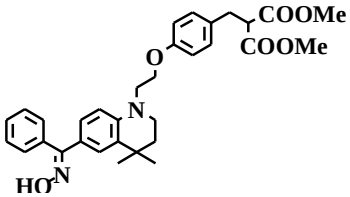	13	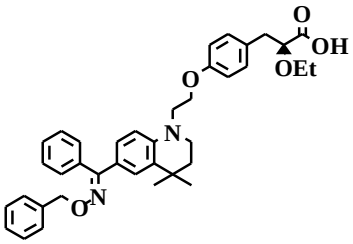
5	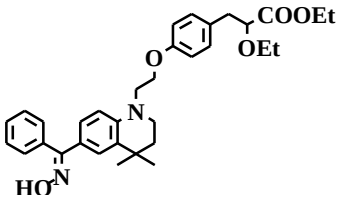	14	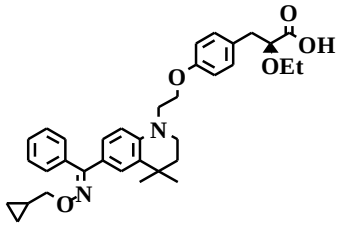

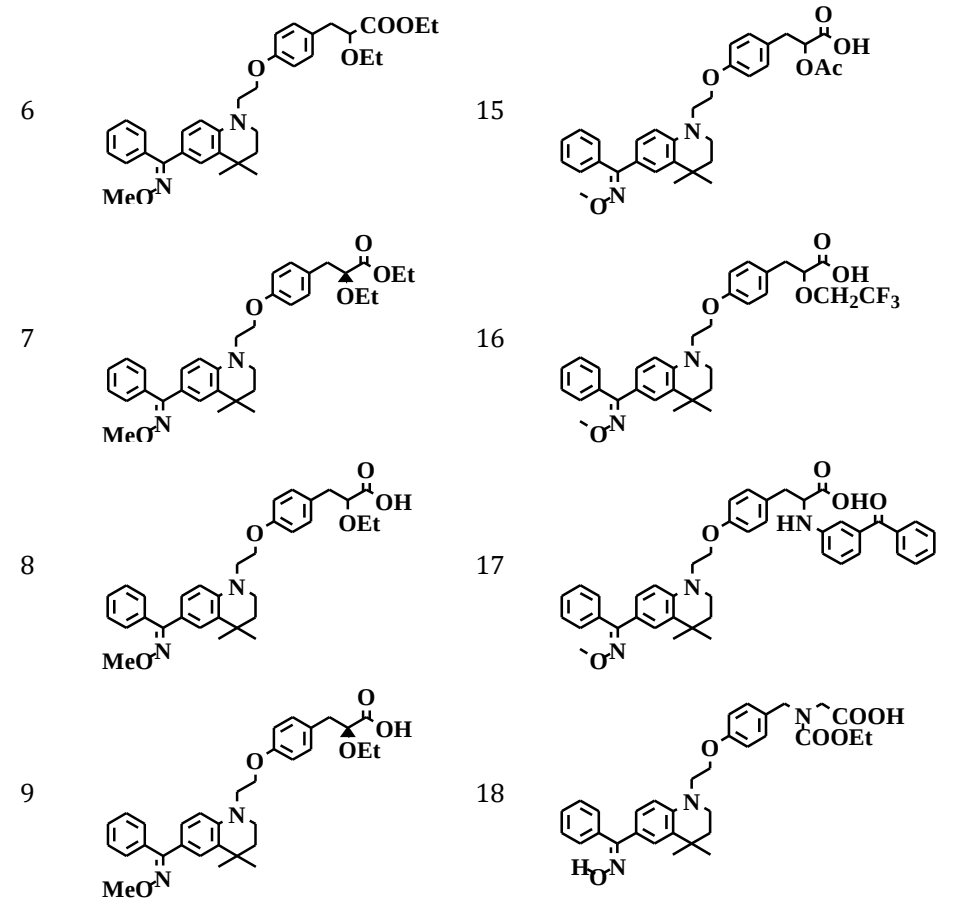

[a]Taken from references[22,23], [b]Rosiglitazone and [c]Tesaglitazar.

These derivatives were evaluated for binding affinity to human PPARγ using a competitive binding assay with [^{3}H] Rosiglitazone. Functional activity was determined in a transient transfection assay using pGAL4hPPARα and pGAL4hPPARγ [22,23].

The reported binding affinity in terms of pK_i(M) and transactivation activity in terms of pEC_{50}(M) of these congeners is presented in Table 3 and Table 6, respectively. For modeling purpose the data set has been sub-divided into training set (for model development) and test set (for external prediction or validation). The selection of test set compounds was made using an in-house written randomization program. The test and training set compounds are mentioned in Table 3.

The structures of the all the compounds (listed in Table 1)were drawn in 2D ChemDraw [24] and subjected to energy minimization in the MOPAC using the AM1 procedure for closed shell system after converting these into 3D modules. The energy minimization was carried out to attain a well-defined conformer relationship among the congeners under study. The molecular descriptors of titled compounds were computed using DRAGON software [25]. This software offers a large number of descriptors corresponding to ten different classes of 0D- to 2D-descriptor modules. The different descriptor classes include the constitutional, topological, molecular walk counts, BCUT descriptors, Galvez topological charge indices, 2D-autocorrelations, functional groups, atom-centered fragments, empirical descriptors and the properties describing descriptors. These descriptors are characteristic to the molecules under multi-descriptor environment. A total number of 486 descriptors, belonging to 0D- to 2D- modules, have been computed to obtain most appropriate models describing the biological activity.

2.2. Model development and validation

A filter based variable selection procedure embedded in the combinatorial protocol in multiple linear regression (CP-MLR) [26] method has been utilized for developing statistical significant models divulging quantitative structure-activity relationship (QSAR). CP-MLR procedure has successfully been applied to obtain QSAR rationales [27-32]. Descriptors which are inter-correlated beyond 0.9 (descriptor *vs.* descriptor, $r > 0.9$) and poorly correlated with biological actions (descriptor vs. activity, $r < 0.1$) has been excluded prior to the application of CP-MLR procedure. In this way the reduced descriptor data set contained 55, 39 and 67 as relevant descriptors for PPARγ binding, and hPPARα

and hPPARγ transactivation activities, respectively. The descriptors have been scaled between the intervals 0 to 1 [33] to ensure that a descriptor will not dominate simply because it has larger or smaller pre-scaled value compared to the other descriptors and the scaled descriptors would have equal potential to influence the QSAR models.

The subdivision of data set into training set and test set have been used, respectively, for model development and external prediction. Goodness of fit of the models was assessed by examining the multiple correlation coefficient (r), the standard deviation (s) and the F-ratio between the variances of calculated and observed activities (F). The internal validation of derived model was ascertained through the cross-validated index, Q^2, from leave-one-out (Q^2_{LOO}) and leave-three-out (Q^2_{L3O}) procedures. The LOO method creates a number of modified data sets by taking away one compound from the parent data set in such a way that each observation has been removed once only. Then one model is developed for each reduced data set, and the response values of the deleted observations are predicted from these models.

The external validation or predictive power of derived model is based on test set compounds. The index r^2_{Test}, representing the squared correlation coefficient between the observed and predicted data of the test-set, has been used to infer the same. A value greater than 0.5 of r^2_{Test} suggests that the model obtained from training set has a reliable predictive power. Chance correlations, if any, associated with the CP-MLR models were explored through randomization test [34, 35] by repeated scrambling of the biological response. Every model has been subjected to 100 such simulation runs. This has been used as a measure to express the percent chance correlation of the model under scrutiny.

To support the findings, a partial least squares (PLS) analysis has been carried out on descriptors identified through CP-MLR. The PLS analysis facilitates the development of a 'single window' structure-activity model and help to categorize the potentiality of identified descriptors in explaining the PPARγ binding profiles of the compounds. It also gives an opportunity to make a comparison of the relative significance among the descriptors. The fraction contributions obtainable from the normalized regression coefficients of the descriptors allow this comparison within the modeled activity.

2.3. Applicability domain

The utility of a QSAR model is based on its accurate predictive ability for new congeners. A model is valid only within its training domain, and new compounds must be assessed as belonging to this domain before the model is applied. The applicability domain is assessed by the leverage values for each compound [36, 37]. A Williams plot (the plot of standardized residuals versus leverage values (h) can then be used for an immediate and simple graphical detection of both the response outliers (Y outliers) and structurally influential chemicals (X outliers) in the model. In this plot, the applicability domain is established inside a squared area within ± β.(standard deviations) and a leverage threshold h*. The threshold h* is generally fixed at 3(k+1)/n (n is the number of compounds in the training-set and k is the number of independent descriptors of the model) whereas β = 2 or 3. Prediction must be considered unreliable for compounds with a high leverage value (h > h*). On the other hand, when the leverage value of a compound is lower than the threshold value, the probability of agreement between predicted and observed values is as high as that for the training set compounds.

3. Results and discussion

3.1. QSAR results

Initially, the pEC_{50} values pertaining to hPPARα and hPPARγ transactivation actions were correlated to pK_i values corresponding to PPARγ binding activity, and pEC_{50} values pertaining to hPPARα and hPPARγ transactivations for all active congeners to confer the diversity between the binding and transactivation activities, and hPPARα and hPPARγ transactivations. The derived correlations are given in Equations (1)-(3).

pK_i (PPARγ) = -0.465 pEC_{50} (hPPARα) + 10.122
n = 13, r = 0.458, s = 0.932, F = 2.927 (1)

pK_i (PPARγ)= 1.051 pEC_{50} (hPPARγ) -1.313
n = 15, r = 0.484, s = 1.052, F = 3.970 (2)

pEC_{50} (hPPARγ) = 0.059 pEC_{50} (hPPARα) +7.362
n = 14, r = 0.138, s = 0.430, F = 0.232 (3)

where n, r, s and F represent respectively the number of data points, the multiple correlation coefficient, the standard deviation and the F-ratio between the variances of calculated and observed activities. All these equations have divulged not very much significant statistical parameters. No correlation between EC_{50} values obtained from transactivation PPARγ tests and K_i values from binding tests suggested that these derivatives may have a binding site different from the Rosiglitazone binding site. This ensures us that the biological actions in terms of binding and or transactivations are independent. Therefore we have considered all types of biological endpoints as the dependent variables in the subsequent parametric analysis.

The PPARγ binding activity of titled compounds was investigated with 55 relevant 0D-, 1D- and 2D-descriptors. A training set consisting 11 compounds was considered for the development of QSAR models and test set involving 04 (nearly one-fourth of the total) compounds for the external validation of derived significant models. CP-MLR resulted one model in one parameter and ten models in two parameters having $r^2_{Test} > 0.5$. These models shared 12 descriptors and are listed in Table 2 along with their physical meaning, average regression coefficient and total incidences. The sign of the regression coefficients indicates the direction of influence of explanatory variables in above models. The positive regression coefficient associated to a descriptor will augment the activity profile of a compound while the negative coefficient will cause detrimental effect to it.

Table 2 Identified descriptors[a] along with their physical meaning, average regression coefficient and incidence[b], in modeling the binding and transactivation activity.

Descriptor; average regression coefficient and (incidence) in analysis for the:		
Binding activity	Transactivation activity	
PPARγ	hPPARα	hPPARγ
Constitutional descriptors (**CONST**):		
MW; -1.458(1)	AMW; -2.340(1)	Me; -0.774 (3)
AMW; 1.565(1),	Me; -1.254(1)	RBN; -1.380(1)
Me; 1.078(1)		
Topological descriptors (**TOPO**):		
MAXDP; -1.529(1)	MAXDP; -1.943(2)	HNar; 1.543 (3)
X2A; 1.826(1)	IC1; -2.188(2)	IVDE; -2.034(1)
T(N..O); -1.760(1)	T(N..N); -2.268(6)	IC2; -1.111(1)
		SIC4; 2.000(1)
2D autocorrelations (**2D-AUTO**):		
GATS4v; 1.478(1)	MATS7m; -1.546(1)	MATS5v; 2.294(3)
GATS2e; -1.508(1)	MATS8m; -1.431(1)	MATS8v; 1.333(1)
	GATS5v; -1.998(1)	MATS5e; -1.393(4)
	GATS6e; 1.326(1)	MATS8e; 1.243(6)
		GATS2e; 0.908(1)
		GATS6e; 1.316(5)
		GATS8e; -1.102(1)
Functional groups (**FUNC**):		
nCconjR; -1.022(1)		nCs; -0.631(1)
nROR; 1.006(1)		nCt; 0.827(1)
nHDon; 2.742(5)		
Atom-centered fragments (**ACF**):		
O-060; -2.424(6)		C-006; -1.035(3)
		C-008; 1.544(8)
Empirical descriptors (**EMP**):		
		Hy; 1.529(1)

[a]The descriptors are identified from the two parameter models for PPARγ binding activity and hPPARα transactivation activity profiles , emerged from CP-MLR protocol with filter-1 as 0.3, filter-2 as 2.0, filter-3 as 0.5 and filter-4 as $0.3 \leq q2 \leq 1.0$ with a training set of 11 and 10 compounds, respectively; and for PPARγ transactivation activity profile three parameter models with filter-1 as 0.3, filter-2 as 2.0, filter-3 as 0.878 and filter-4 as

0.3 ≤ q2 ≤1.0 with a training set of 13 compounds. [b]The average regression coefficient of the descriptor corresponding to all models and the total number of its incidence. The arithmetic sign of the coefficient represents the actual sign of the regression coefficient in the models. CONST: MW, molecular weight; AMW; average molecular weight; Me, mean atomic Sanderson electronegativity (scaled on Carbon atom); RBN, number of rotatable bonds; TOPO: MAXDP maximal electrotopological positive variation; X2A, average connectivity index chi-2; T(N..O), sum of topological distances between N..O; T(N..N), sum of topological distances between N..N; HNar, Narumi harmonic index; IVDE, mean information content vertex degree equality; IC1, information content index (neighborhood symmetry of 1-order); IC2, information content index (neighborhood symmetry of 2-order); SIC4, structural information content (neighborhood symmetry of 4-order); 2D-AUTO: MATS7m, Moran autocorrelation of lag-7/ weighted by atomic masses; MATS8m, Moran autocorrelation of lag-7/ weighted by atomic masses; MATS5v, Moran autocorrelation of lag-5/ weighted by atomic van der Waals volumes; MATS8v, Moran autocorrelation of lag-8/ weighted by atomic van der Waals volumes; MATS5e, Moran autocorrelation of lag-5/ weighted by atomic Sanderson electronegativities; MATS8e, Moran autocorrelation of lag-8/ weighted by atomic Sanderson electronegativities; GATS4v, Geary autocorrelation of lag-4/ weighted by atomic van der Waals volumes; GATS5v, Geary autocorrelation of lag-5/ weighted by atomic van der Waals volumes; GATS2e, Geary autocorrelation of lag-2/ weighted by atomic Sanderson electronegativities; GATS6e, Geary autocorrelation of lag-6/ weighted by atomic Sanderson electronegativities; GATS8e, Geary autocorrelation of lag-8/ weighted by atomic Sanderson electronegativities; FUNC: nCconjR; number of exo-conjugated C(sp2); nROR; number of aliphatic ethers; nHDon; number of donor atoms for H-bonds (with N and O); nCs; number of total secondary C(sp3); nCt; number of total tertiary C(sp3); ACF: O-060, Al-O-Ar/Ar-O-Ar/R..O..R/R-O-C=X; C-006, CH2RX; C-008, CHR2X; EMP: Hy, hydrophilic factor.

The selected highly significant two parameter models, emerged in CP-MLR for the PPARγ binding activity are given below.

pK_i= -1.529(0.437)MAXDP + 2.379(0.394)nHDon + 6.328
n = 11, r = 0.940, s = 0.455, F = 30.721, q^2_{LOO} = 0.811, q^2_{L3O} = 0.781, r^2_{Test}= 0.791 (4)

pK_i= 1.006(0.295)nROR + 2.952(0.396)nHDon + 4.866
n = 11, r = 0.938, s = 0.462, F = 29.711, q^2_{LOO} = 0.764, q^2_{L3O} = 0.784, r^2_{Test}= 0.662 (5)

pK_i= 1.826(0.534)X2A – 2.258(0.378)O-060 + 7.011
n = 11, r = 0.934, s = 0.478, F = 27.460, q^2_{LOO} = 0.813, q^2_{L3O} = 0.810, r^2_{Test}= 0.603 (6)

pK_i= 1.565(0.479)AMW – 2.295(0.387)O-060 + 6.892
n = 11, r = 0.930, s = 0.491, F = 25.847, q^2_{LOO} = 0.740, q^2_{L3O} = 0.706, r^2_{Test}= 0.725 (7)

The data within the parentheses are the standard errors associated with regression coefficients. The descriptors, participated in above models, are from constitutional (AMW), topological (MAXDP and X2A), functional group (nHDon and nROR) and atom-centered fragment (O-060) class. Constitutional class descriptors are molecular connectivity and conformations independent 0D descriptors. The emerged constitutional class descriptor AMW (average molecular weight) has shown positive correlation to activity favoring high average molecular weight of a molecule for elevated binding activity. Topological class descriptors are based on a graph representation of the molecule and are numerical quantifiers of molecular topology obtained by the application of algebraic operators to matrices representing molecular graphs and whose values are independent of vertex numbering or labeling. They can be sensitive to one or more structural features of the molecules such as size, shape, symmetry, branching and cyclicity and can also encode chemical information concerning atom type and bond multiplicity. The negative contribution of descriptor MAXDP (maximal electrotopological positive variation) and positive contribution of descriptor X2A (average connectivity index, chi-2) suggested that a lower value of descriptor MAXDP and a higher value of X2A would be supportive to the activity.

Descriptors nHDon and nROR are functional group class descriptors. Descriptor nHDon represents number of donor atoms for H-bonds (with N and O) and nROR corresponds to number of aliphatic ethers. Presence and or higher number of both the types of functionality in a molecular structure would be favorable to the binding activity. Descriptor O-060 is representative of atom centered fragments (ACF) class. ACF class descriptors are based on the counting of 120 atom centered fragments, defined by Ghose-Crippen in a molecular structure. Descriptor O-060 represents Al-O-Ar/Ar-O-Ar/R..O..R/R-O-C=X type fragments in a molecular structure. The negative sign of correlation coefficient of this descriptor recommends absence of such types of fragments for elevated PPARγ binding profile. Based on the total number of incidences, it is also clear that descriptors O-060 and nHDon appeared as most relevant descriptors to explain the binding profiles of titled compound (Table 2).

In above equations (4) to (7), the F-values are significant at 99% level. Value greater than 0.5 of both the indices q^2_{LOO} and q^2_{L3O} showed internal robustness of the models whereas accountability of selected test-set for external validation reflected through the r^2_{Test} values (> 0.5). These models are able to estimate up to 88.36 percent of variance in observed activity of the compounds. The derived statistical parameters of these four models in two parameters have shown the statistically significance, therefore, these models were used to calculate the PPARγ binding activity profiles of all the compounds and are included in Table 3 for the sake of comparison with observed ones.

Table 3 Observed, calculated and predicted PPARγ binding activities of Tetrahydroquinolines.

Cpd.	pK_i (M)[a]										
	Obsd[b].	Eq. (4)		Eq. (5)		Eq. (6)		Eq. (7)		PLS	
		Calc.	Pred[c].	Calc.	Pred[c].	Calc.	Pred[c].	Calc.	Pred[c].	Calc.	Pred[c].
1	8.10	8.35	8.47	7.82	7.60	7.69	7.61	8.46	8.83	8.16	8.19
2	7.74	7.52	7.46	7.35	7.28	7.71	7.45	7.02	6.66	7.55	7.18
3	5.00	4.80	4.62	4.87	4.76	4.80	4.68	5.08	5.13	4.83	4.74
4	5.00	5.67	5.85	4.87	4.76	4.75	4.58	5.09	5.15	5.28	5.37
5	6.21	5.51	5.32	5.87	5.77	6.04	6.01	5.84	5.75	5.70	5.59
6	5.00	5.50	5.63	5.87	6.14	6.09	6.24	5.75	5.95	5.57	5.71
7[d]	5.00	5.50	-[d]	5.87	-[d]	6.09	-[d]	5.75	-[d]	5.57	-[d]
8[d]	7.32	7.34	-[d]	7.35	-[d]	7.27	-[d]	7.07	-[d]	7.13	-[d]
9[e]	-[e]	-[e]	-[e]	-[e]	-[e]	-[e]	-[e]	-[e]	-[e]	-[e]	-[e]
10	7.05	7.34	7.39	7.35	7.41	7.27	7.32	7.07	7.08	7.13	7.14
11[d]	7.74	7.34	-[d]	7.35	-[d]	7.27	-[d]	7.07	-[d]	7.13	-[d]
12	7.27	7.32	7.33	7.35	7.36	7.38	7.40	7.05	6.98	7.19	7.17
13	7.74	7.29	7.22	7.35	7.28	7.32	7.24	7.16	7.02	7.21	7.11
14[d]	6.60	7.31	-[d]	7.35	-[d]	7.17	-[d]	6.97	-[d]	7.15	-[d]
15[e]	-[e]	-[e]	-[e]	-[e]	-[e]	-[e]	-[e]	-[e]	-[e]	-[e]	-[e]
16	7.48	7.28	7.25	7.35	7.32	7.74	7.80	7.86	7.96	7.92	8.04
17	7.27	7.29	7.34	7.82	8.24	7.06	7.00	7.48	7.52	7.33	7.38
18[e]	-[e]	-[e]	-[e]	-[e]	-[e]	-[e]	-[e]	-[e]	-[e]	-[e]	-[e]

[a]On molar basis, K_i represents the binding affinity to human PPARγ using a competitive binding assay with an appropriate radioligand[^{3}H]Rosiglitazone; [b]Taken from ref. [22,23]; [c]Leave-one-out (LOO) procedure; [d]Compound included in test set and [e]Compound with uncertain activity, not part of data set.

A close agreement between them has been observed. Additionally, the graphical display, showing the variation of observed versus calculated activities is given in Figure 1 to ensure the goodness of fit for each of these four models.

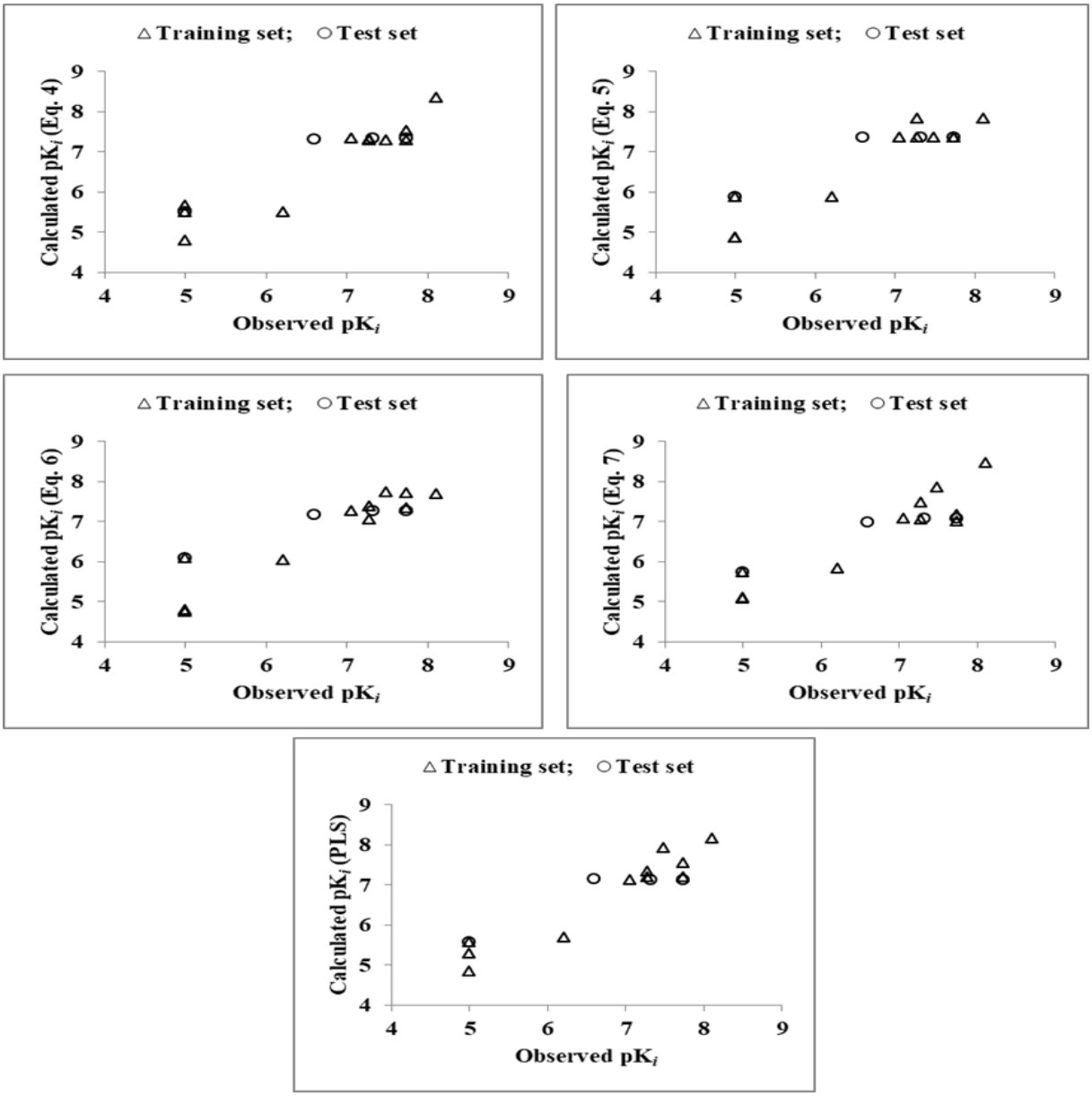

Figure 1 Plot of observed and calculated pK$_i$values for training- and test-set compounds**.**

A PLS analysis has also been carried out on 12 descriptors (identified through CP-MLR) to support the study. The results of PLS analysis are given in Table 4. For this purpose, the descriptors have been autoscaled (zero mean and unit s.d.) to give each one of them equal weight in the analysis. In the PLS cross-validation, two components have been found to be the optimum for these 12 descriptors and they explained 91.4 percent variance in the activity ($r^2 = 0.914$).The MLR-like PLS coefficients of these 12 descriptors are given in Table 4.

Table 4 PLS and MLR-like PLS models from the descriptors of two parameter CP-MLR models for PPARγ binding affinity.

A: PLS equation			
PLS components	PLS coefficient (s.e.)[a]		
Component-1	0.483(0.057)		
Component-2	0.306(0.077)		
Constant	6.714		
B: MLR-like PLS equation			
S. No.	Descriptor	MLR-like coefficient (f.c.)[b]	Order
1	MW	0.025(0.017)	10
2	AMW	0.118(0.082)	4
3	Me	0.071(0.049)	7
4	MAXDP	-0.167(-0.116)	3
5	X2A	0.103(0.071)	5
6	T(N..O)	0.020(0.014)	11
7	GATS4v	-0.025(-0.018)	9
8	GATS2e	-0.087(-0.060)	6
9	nCconjR	-0.020(-0.014)	12
10	nROR	0.070(0.048)	8
11	nHDon	0.364(0.252)	2
12	O-060	-0.376(-0.260)	1
Constant		6.529	
C: PLS regression statistics		**Values**	
n		11	
r		0.956	
s		0.392	
F		42.800	
q^2_{LOO}		0.850	
q^2_{L30}		0.887	
r^2_{Test}		0.762	

[a]Regression coefficient of PLS factor and its standard error. [b]Coefficients of MLR-like PLS equation in terms of descriptors for their original values; f.c. is fraction contribution of regression coefficient, computed from the normalized regression coefficients obtained from the auto scaled (zero mean and unit s.d.) data.

The calculated activity values of training- and test-set compounds are in close agreement to that of the observed ones and are listed in Table 3. For the sake of comparison, the plot between observed and calculated activities (through PLS analysis) for the training- and test-set compounds is given in Figure 1. Figure 2 shows a plot of the fraction contribution of normalized regression coefficients of these descriptors to the activity (Table 4).

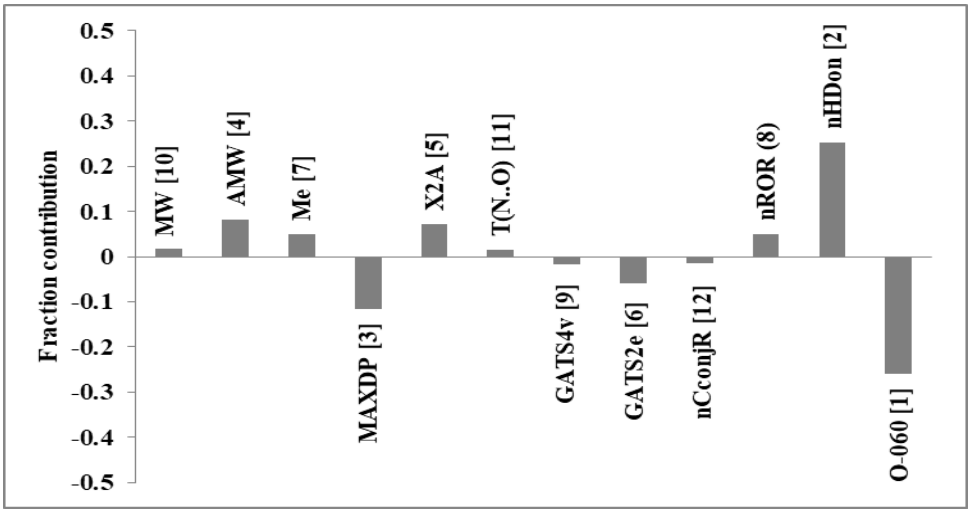

Figure 2 Plot of fraction contribution of MLR-like PLS coefficients (normalized) against 12 identified descriptors (Table 4) associated with PPARγ binding affinity of the compounds.

Descriptors in decreasing order of significance in PLS analysis are O-060, nHDon, MAXDP, AMW, X2A, GATS2e, Me, nROR, GATS4v, MW, T(N..O) and nCconjR. Among these descriptors, O-060, nHDon, MAXDP, AMW, X2A and nROR are part of Equations discussed above and convey same inferences in PLS analysis. The positive contributions of constitutional class descriptors MW (molecular weight) and Me (mean atomic Sanderson electronegativity scaled on Carbon atom); and topological class descriptor T(N..O), representing the sum of topological distances between N and O atoms advocated that higher values of these are helpful in improving the activity profile. Whereas lower values of descriptors GATS4v (Geary autocorrelation of lag-4/ weighted by atomic van der Waals volumes), GATS2e (Geary autocorrelation of lag-2/ weighted by atomic Sanderson electronegativities) and number of exo-conjugated C(sp2) (descriptor nCconjR) would be supportive to enhance the activity. It is also observed that PLS model from the dataset devoid of 12 descriptors (Table 4) remained inferior in explaining the activity of the analogues.

QSAR rationales, with the same test-set used earlier for the analysis of PPARγ binding activity, have also been obtained for other reported activity profile pertaining to hPPARα and hPPARγ transactivation. A descriptor pool of 39 and 67 relevant descriptors for hPPARα and hPPARγ transactivation, respectively, were subjected to CP-MLR analysis. CP-MLR resulted a total number of 08 models in two parameters sharing 9 descriptors for hPPARα activity. For the hPPARγ activity 15 three parameters models sharing 18 descriptors were obtained. The shared descriptors along with their physical meaning, average regression coefficient and total incidences for both the analysis have been given in Table 2. The selected models emerged through CP-MLR are mentioned below.

pEC_{50}(hPPARα)= – 1.686(0.388)IC1 – 1.933(0.396)T(N..N) + 7.965
n = 10, r = 0.945, s = 0.355, F = 29.412, q^2_{LOO} = 0.837, q^2_{L30} = 0.847, r^2_{Test}= 0.610 (8)

pEC_{50}(hPPARα)= – 2.013(0.469)MAXDP – 2.690(0.426)IC1 + 8.450
n = 10, r = 0.933, s = 0.391, F = 23.596, q^2_{LOO} = 0.740, q^2_{L30} = 0.707, r^2_{Test}= 0.749 (9)

pEC_{50}(hPPARα)= – 2.340(0.422)AMW – 1.874(0.517)MAXDP + 7.881
n = 10, r = 0.916, s = 0.435, F = 18.364, q^2_{LOO} = 0.643, q^2_{L30} = 0.571, r^2_{Test}= 0.765 (10)

pEC_{50}(hPPARα)= – 1.976(0.518)T(N..N) – 1.546(0.540)MATS7m + 7.995
n = 10, r = 0.905, s = 0.462, F = 15.876, q^2_{LOO} = 0.724, q^2_{L30} = 0.700, r^2_{Test}= 0.617 (11)

Newly appeared descriptors IC1 and T(N..N) are topological class descriptors whereas descriptor MATS7m belong to 2D-autocorrelations (2D-AUTO) class. The 2D-AUTO descriptors, ATSke, GATSke and MATSke have their origin in autocorrelation of topological structure of Broto-Moreau, of Moran and of Geary, respectively. The computation of these descriptors involves the summation of different autocorrelation functions corresponding to the different fragment lengths and lead to different autocorrelation vectors corresponding to the lengths of the structural fragments. Also a weighting component in terms of a physicochemical property has been embedded in these descriptors. As a result, these descriptors address the topology of the structure or parts thereof in association with a selected physicochemical

property. In these descriptors' nomenclature, the penultimate character, a number, indicates the number of consecutively connected edges considered in its computation and is called as the autocorrelation vector of lag k (corresponding to the number of edges in the unit fragment). The very last character of the descriptor's nomenclature indicates the physicochemical property considered in the weighting component – m for atomic mass, e for atomic Sanderson electronegativity and p for atomic polarizability - for its computation.

All the descriptors, participated in Eqs. (8) to (11), have shown negative correlation to activity as evinced from the signs of the correlation coefficients thus lower values of information content index of 1st order neighborhood symmetry (descriptor IC1), sum of topological distances between N..N (descriptor T(N..N)), maximal electrotopological positive variation (descriptor MAXDP), average molecular weight (descriptor AMW) and Moran autocorrelation of lag-7/ weighted by atomic masses (descriptor MATS7m) would be beneficiary to the hPPARα activity.

The derived statistical parameters models have revealed that these models are statistically significant. The values greater than 0.5 of indices q^2_{LOO} and q^2_{L30} have accounted the internal robustness of models and the r^2_{Test} values greater than 0.5 are accountable for external validation.

These models are able to estimate up to 89.36 percent of variance in observed activity of the compounds. These models were, therefore, used to calculate the activity profiles of all the compounds and are included in Table 5 for the sake of comparison with observed ones. A close agreement between them has been observed.

Table 5 Observed and calculated transactivation activities of Tetrahydroquinoline analogues.

Cpd.	Transactivation pEC_{50}(M)[a]									
	hPPARα					hPPARγ				
	Obsd.[b]	Calculated				Obsd.[b]	Calculated			
		Eq.(8)	Eq.(9)	Eq.(10)	Eq.(11)		Eq.(12)	Eq.(13)	Eq.(14)	Eq.(15)
1	5.00	5.01	5.58	5.10	5.04	8.40	8.31	8.62	8.14	8.48
2	6.38	6.71	6.44	5.98	6.91	7.43	7.34	7.57	7.71	7.23
3	-[c]	7.81	6.19	5.28	7.76	6.82	7.35	6.75	6.87	7.17
4	-[c]	6.73	6.19	6.33	7.32	6.71	6.56	6.44	6.55	6.74
5	6.72	7.19	6.71	6.74	7.16	7.32	7.03	7.51	7.70	7.02
6	7.52	7.60	7.35	6.86	7.01	7.72	7.44	7.58	7.76	7.32
7[d]	7.54	7.60	7.35	6.86	7.01	7.85	7.44	7.58	7.76	7.32
8[d]	7.92	6.91	7.11	7.39	6.70	7.96	7.45	7.49	7.69	7.54
9	7.54	6.91	7.11	7.39	6.70	7.85	7.45	7.49	7.69	7.54
10	6.71	6.91	7.11	7.39	6.70	7.19	7.45	7.49	7.69	7.54
11[d]	6.94	6.91	7.11	7.39	6.70	8.11	7.45	7.49	7.69	7.54
12	7.14	6.87	7.03	7.41	7.32	7.89	7.90	7.52	7.69	7.74
13	7.47	7.30	7.67	7.20	7.47	8.15	8.34	7.85	7.66	8.52
14[d]	8.05	7.04	7.28	7.51	7.63	8.12	7.98	7.85	7.68	7.88
15	-[c]	6.51	6.48	6.93	6.54	-[c]	7.10	7.23	7.59	7.43
16	6.00	5.92	5.44	6.14	6.08	6.90	7.23	6.87	6.69	6.71
17	5.00	5.07	5.04	5.26	5.09	7.85	7.72	8.19	7.96	7.90
18	-[c]	4.84	5.34	6.19	5.22	5.00	5.09	5.34	5.11	5.33

[a]On molar basis, determined in a transient transfection assay using pGAL4hPPAR and pGAL4hPPARγ; [b]Taken from ref. [22,23]; [c]Inactive compound, not part of data set and [d]Compound included in test set.

Considering the number of observation in the data set for the hPPARγ transactivation profile, models with up to three descriptors were explored. Following are the selected three-descriptor models, obtained from CP-MLR, for the hPPARγ transactivation.

pEC_{50}(hPPARγ)= 2.386(0.312)MATS5v + 1.369(0.237)MATS8e + 0.827(0.241)nCt + 4.807
n = 13, r = 0.950, s = 0.311, F = 28.279, q^2_{LOO} = 0.640, q^2_{L30} = 0.713, r^2_{Test}= 0.545 (12)

pEC_{50}(hPPARγ)= 1.089(0.346)HNar + 1.129(0.232)MATS8e + 1.363(0.213)C-008 + 5.156
n = 13, r = 0.950, s = 0.313, F = 27.929, q^2_{LOO} = 0.736, q^2_{L3O} = 0.760, r^2_{Test}= 0.613 (13)

pEC_{50}(hPPARγ)= – 0.710(0.242)Me + 1.090(0.240)MATS8e + 1.595(0.215)C-008 + 5.808
n = 13, r = 0.946, s = 0.325, F = 25.748, q^2_{LOO} = 0.785, q^2_{L3O} = 0.701, r^2_{Test}= 0.766 (14)

pEC_{50}(hPPARγ)= 2.482(0.329)MATS5v + 1.390(0.308)GATS6e – 0.983(0.231)C-006 + 5.707
n = 13, r = 0.946, s = 0.325, F = 25.723, q^2_{LOO} = 0.709, q^2_{L3O} = 0.808, r^2_{Test}= 0.560 (15)

In all above equations (12) to (15) the F-values remained significant at 99% level. The values, greater than 0.5, obtained for the indices q^2_{LOO}, q^2_{L3O}, and r^2_{Test} ascertained the internal robustness and external validation of the models.

These models are capable to explain up to 90.40 percent of variance in observed activity of the compounds. The derived statistical parameters are in tune to statistical significance. The activity profiles of all the compounds calculated using these equations are in close agreement to the observed ones and the same are included in Table 5.

2D-autocorrelations class descriptors MATS5v (Moran autocorrelation of lag-5/ weighted by atomic van der Waals volumes), MATS8e (Moran autocorrelation of lag-8/ weighted by atomic Sanderson electronegativities) and GATS6e (Geary autocorrelation of lag-6/ weighted by atomic Sanderson electronegativities) added positively to the inhibitory activity suggesting that a higher values of descriptors MATS5v, MATS8e and GATS6e would be helpful to augment the activity. Constitutional class descriptors Me (mean atomic Sanderson electronegativity scaled on Carbon atom) favors low value of mean atomic Sanderson electronegativity for elevated activity.

Descriptor HNar, corresponds to Narumi harmonic index, is a topological class descriptor. The positive contribution of descriptor HNar suggested that a higher value of it would be supportive to the activity. The other participated descriptors are nCt (from the functional group class), and C-006 and C-008 (from the atom-centered fragments). Number of total tertiary C(sp3) (descriptor nCt) and CHR2X type atom centered fragment (descriptor C-008) correlated positively to the activity suggested that a higher value of these will augment the activity. On the other hand negative correlation of descriptor C-006 advocated that CH2RX type structural fragments would be detrimental to the activity.

3.2. Applicability domain

On analyzing the applicability domain (AD) in the Williams plot (Figure 3) of the model based on the whole dataset (Table 7), none of the compound has been identified as an obvious 'outlier' for the PPARγ binding activity if the limit of normal values for the Y outliers (response outliers) was set as 3×(standard deviation) units.

Table 7 Models derived for the whole data set (n = 15) for the PPARγ binding affinity in descriptors identified through CP-MLR.

Model	r	s	F	q^2_{LOO}	Eq.
pKi = -1.523(0.412)MAXDP +2.483(0.378)nHDon + 6.229	0.930	0.457	38.897	0.808	(4a)
pKi = 0.915(0.296)nROR + 3.123(0.401)nHDon + 4.780	0.916	0.499	31.601	0.739	(5a)
pKi = 1.962(0.579)X2A – 2.374(0.386)O-060 + 6.938	0.904	0.534	26.829	0.745	(6a)
pKi = 1.668(0.441)AMW – 2.457(0.363)O-060 + 6.894	0.914	0.505	30.802	0.727	(7a)

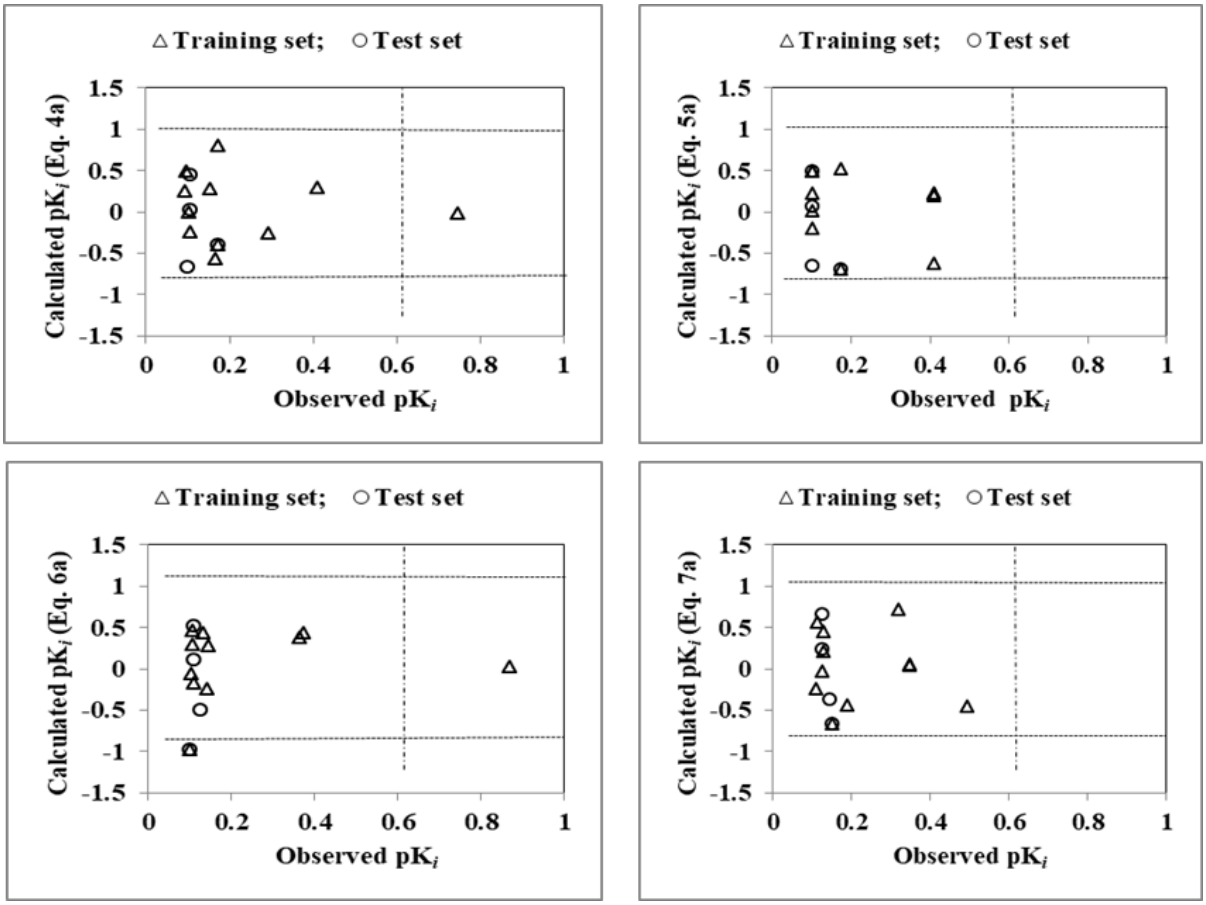

Figure 3 Williams plot for the training-set and test- set for binding affinity of PPARγ for the compounds in Table 1. The horizontal dotted line refers to the residual limit (±3×standard deviation) and the vertical dotted line represents threshold leverage h* (= 0.6).

Compounds **2** and **17** found to have leverage (h) values greater than the threshold leverage (h*) suggesting them as chemically influential compounds. For both the training-set and test-set, the suggested model matches the high quality parameters with good fitting power and the capability of assessing external data. Furthermore, all of the compounds were within the applicability domain of the proposed model and were evaluated correctly.

4. Conclusion

This study has provided a rational approach for the development of tetrahydroquinoline derivatives as PPARα/γ agonists**.** The descriptors identified in CP-MLR analysis for the PPARγ binding activity have highlighted the role of average molecular weight (AMW), maximal electrotopological positive variation (MAXDP), average connectivity index i.e. chi-2 (X2A) to explain the binding actions in addition to presence of donor atoms for H-bonds with N and O (nHDon), aliphatic ethers (nROR) and absence of Al-O-Ar/Ar-O-Ar/R..O..R/R-O-C=X type fragments in a molecular structure (O-060) have also shown prevalence to optimize the PPARγ binding activity of titled compounds. PLS analysis has further confirmed the dominance of the CP-MLR identified descriptors and applicability domain analysis revealed that the suggested model for PPARγ binding activity matches the high quality parameters with good fitting power and the capability of assessing external data and all of the compounds was within the applicability domain of the proposed model and were evaluated correctly.

Derived statistical significant models for hPPARα transactivation activity revealed that lower values of information content index of 1st order neighborhood symmetry (descriptor IC1), sum of topological distances between N..N (descriptor T(N..N)), maximal electrotopological positive variation (descriptor MAXDP), average molecular weight (descriptor AMW) and Moran autocorrelation of lag-7/ weighted by atomic masses (descriptor MATS7m) would be beneficiary to the hPPARα activity. Role of atomic van der Waals volumes and electronegativities to explain the hPPARγ transactivation activity is evinced through participation of descriptors MATS5v, MATS8e, GATS6e and Me. Additionally

a higher value of Narumi harmonic index (HNar), number of total tertiary C(sp3) (descriptor nCt), presence of CHR2X type atom centered fragment (descriptor C-008) and absence of CH2RX type structural fragments (descriptor C-006) will augment the hPPARγ transactivation activity.

Compliance with ethical standards

Acknowledgments

Authors are thankful to their institution for providing necessary facilities to complete this study.

Disclosure of conflict of interest

The authors declare no conflict of interest.

References

[1] Saltiel AR. (2001). New perspectives into the molecular pathogenesis and treatment of type 2 diabetes. Cell, 104, 517-529.

[2] Zimmet P, Alberti KG and Shaw J. (2001). Global and societal implications of the diabetes epidemic. Nature, 414, 782-787.

[3] Moller DE. (2001). New drug targets for type 2 diabetes and the metabolic syndrome. Nature, 414, 821-827.

[4] Mangelsdorf DJ and Evans RM. (1995). The RXR heterodimers and orphan receptors. Cell, 83, 841-850.

[5] Isseman I and Green S. (1990). Activation of a member of the steroid hormone receptor superfamily by peroxisome proliferators. Nature, 347, 645-650.

[6] Berger J and Moller DE. (2002). The mechanisms of action of PPARs. Annual Review of Medicine. 53, 409-435.

[7] Staels B and Fruchart J-C. (2005). Therapeutic roles of peroxisome proliferator-activated receptor agonists. Diabetes, 54, 2460-2470.

[8] Berger JP, Akiyama TE and Meinke PT. (2005). PPARs: Therapeutic targets for metabolic disease. Trends in Pharmacological Sciences, 26, 244-251.

[9] Willson TM, Brown PJ, Sternbach DD and Henke BR. (2000). The PPARs: From orphan receptors to drug discovery. Journal of Medicinal Chemistry, 43, 527-550.

[10] Henke BR. (2004). Peroxisome proliferator-activated receptor alpha/gamma dual agonists for the treatment of type 2 diabetes. Journal of Medicinal Chemistry, 47, 4118-4127.

[11] Lehmann JM, Moore MB, Smith-Oliver TA, Wilkinson WO, Willson TM and Kliewer SA. (1995). An antidiabetic thiazolidinedione is a high affinity ligand for peroxisome proliferator-activated receptor gamma (PPAR gamma). The Journal of Biological Chemistry, 270, 12953-12956.

[12] Willson TM, Cobb JE, Cowan DJ, Wiethe RW, Correa ID, Prakash SR, Beck KD, Moore LB, Kliewer SA and Lehmann JM. (1996). The structure-activity relationship between peroxisome proliferator-activated receptor gamma agonism and the antihyperglycemic activity of thiazolidinediones. Journal of Medicinal Chemistry, 39, 665-668.

[13] Lohray BB, Lorhay VB, Bajji AC, Kalchar S, Poondra RR, Padakanti S, Chakrabarti R,Vikramadithyan RK, Misra P, Juluri S, Mamidi RNVS and Rajagopalan R. (2001). (-)3-[4-[2-(Phenoxazin-10-yl)ethoxy]phenyl ethoxypropanoic acid [(-)DRF 2725]: A dual PPAR agonist with potent antihyperglycemic and lipid modulating activity. Journal of Medicinal Chemistry, 44, 2675-2678.

[14] Sauerberg P, Petterson I, Jeppesen L, Bury PS, Mogensen JP, Wassermann K, Brand CL, Sturis J, Wöldike HF, Fleckner J, Anderson AST, Mortensen SB, Anders-Svensson L,Rasmussen HB, Lehmann SV, Polivka Z, Sindelar K, Panajotova V, Ynddal L and Wulff EM. (2002). Novel tricyclic-alpha-alkyloxyphenylpropionic acids: Dual PPARalpha/gamma agonists with hypolipidemic and antidiabetic activity. Journal of Medicinal Chemistry, 45, 789-804.

[15] Ebdrup S, Petterson I, Rasmussen HB, Deussen HJ, Frost-Jensen A, Mortensen SB, Fleckner J, Pridal L, Nygaard L and Sauerberg P. (2003). Synthesis and biological and structural characterization of the dual-acting peroxisome

proliferator-activated receptor alpha/gamma agonist Ragaglitazar. Journal of Medicinal Chemistry, 46, 1306-1317.

[16] Devasthale PV, Chen S, Jeon Y, Qu F, Shao C, Wang W, Zhang H, Farreley D, Golla R, Grover G, Harrity T, Ma Z, Moore L, Ren J, Seethala R, Cheng L, Sleph P, Sun W, Tieman A, Wetterau JR, Doweyko A, Chandrasena G, Chang SY, Humphreys JR,Sasseville VG, Biller SA, Ryono DE, Selan F, Harihanan N and Cheng PTW. (2005). Design and synthesis of N-[(4-methoxyphenoxy)carbonyl]-N-[[4-[2-(5-methyl-2-phenyl-4-oxazolyl)ethoxy]phenyl] methyl] glycine [Muraglitazar/BMS-298585], a novel peroxisome proliferator-activated receptor alpha/gamma dual agonist with efficacious glucose and lipid-lowering activities. Journal of Medicinal Chemistry, 48, 2248- 2250.

[17] Koyama H, Miller DJ, Boueres JK, Desai RC, Jones AB, Berger JP, MacNaul KL, Kelly LJ, Doebber TW, Wu MS, Zhou G, Wang PR, Ippolito MC, Chao YS, Agrawal AK, Franklin R, Heck JV, Wright SD, Moller DE and Sahoo SP. (2004). (2R)-2-Ethylchromane-2-carboxylic acids: Discovery of novel PPARalpha/gamma dual agonistsas antihyperglycemic and hypolipidemic agents. Journal of Medicinal Chemistry, 47, 3255-3263.

[18] Shi GQ, Dropinski JF, McKeever BM, Xu S, Becker JW, Berger JP, MacNaul KL, Elbrecht A, Zhou G, Doebber TW, Wang P, Chao YS, Forrest M, Heck JV, Moller DE and Jones AB. (2005). Design and synthesis of alpha-Aryloxyphenylacetic acid derivatives: A Novel class of PPARalpha/gamma dual agonists with potent antihyperglycemic and lipid modulating activity. Journal of Medicinal Chemistry, 48, 4457-4468.

[19] Gervois P, Fruchart J-C and Staels B. (2004). Inflammation, dyslipidaemia, diabetes and PPARs: Pharmacological interest of dual PPARalpha and PPARgamma agonists. The International Journal of Clinical Practice, 58, 22-29.

[20] Berger JP, Akiyama TE and Meinke PT. (2005). PPARs: Therapeutic targets for metabolic disease. Trends in Pharmacological Sciences, 26, 244-251.

[21] Parmenon C, Viaud-Massuard M-C, Guillard J, Dacquet C, Ktorza A and Caignard D-H. (2006). WO2006/079719.

[22] Parmenon C, Guillard J, Caignard D-H, Hennuyer N, Staels B, Audinot-Bouchez V, Boutin J-A, Ktorza A, Dacquet C and Viaud-Massuard M-C. (2008). 4,4-Dimethyl-1,2,3,4-tetrahydroquinoline-based PPARα/γ agonists. Part I: Synthesis and pharmacological evaluation. Bioorganic and Medicinal Chemistry Letters, 18, 1617-1622.

[23] Parmenon C, Guillard J, Caignard D-H, Hennuyer N, Staels B, Audinot-Bouchez V, Boutin J-A, Dacquet C, Ktorza A and Viaud-Massuard M-C. (2009). 4,4-Dimethyl-1,2,3,4- tetrahydroquinoline-based PPARα/γ agonists. Part. II: Synthesis and pharmacological evaluation of oxime and acidic head group structural variations Bioorganic and Medicinal Chemistry Letters, 19, 2683–2687.

[24] ChemDraw Ultra 6.0 and Chem3D Ultra, Cambridge Soft Corporation, Cambridge, USA.

[25] Todeschini R and Consonni V. Dragon software (version 1.11-2001), Milano, Italy.

[26] Prabhakar YS. (2003). A combinatorial approach to the variable selection in multiple linear regression: analysis of Selwood et al. Data Set-a case study. QSAR and Combinatorial Science, 22, 583-595.

[27] Sharma S, Prabhakar YS, Singh P and Sharma BK. (2008). QSAR study about ATP-sensitive potassium channel activation of cromakalim analogues using CP-MLR approach. European Journal of Medicinal Chemistry, 43, 2354-2360 .

[28] Sharma S, Sharma BK, Sharma SK, Singh P and Prabhakar YS. (2009). Topological descriptors in modeling the agonistic activity of human A3 adenosine receptor ligands: The derivatives of 2-Chloro-N6-substituted-4'-thioadenosine-5'-uronamide. European Journal of Medicinal Chemistry, 44, 1377-1382.

[29] Sharma BK, Pilania P, Singh P and Prabhakar YS. (2010). Combinatorial protocol in multiple linear regression/partial least-squares directed rationale for the caspase-3 inhibition activity of isoquinoline-1,3,4-trione derivatives. SAR and QSAR in Environmental Research, 21, 169-185 .

[30] Sharma BK, Singh P, Sarbhai K and Prabhakar YS. (2010). A quantitative structure-activity relationship study on serotonin 5-HT6 receptor ligands: Indolyl and piperidinyl sulphonamides. SAR and QSAR in Environmental Research, 21, 369-388 .

[31] Sharma BK, Pilania P, Sarbhai K, Singh P and Prabhakar YS. (2010). Chemometric descriptors in modeling the carbonic anhydrase inhibition activity of sulfonamide and sulfamate derivatives. Molecular Diversity, 14, 371-384.

[32] Sharma BK, Singh P, Shekhawat M, Sarbhai K and Prabhakar YS. (2011). Modelling of serotonin reuptake inhibitory and histamine H3 antagonistic activity of piperazine and diazepane amides: QSAR rationales for co-optimization of the activity profiles., SAR and QSAR in Environmental Research, 22, 365-383.

[33] Golbraikh A and Tropsha A. (2002). Beware of q^2! Journal of Molecular Graphics and Modeling, 20, 269-276.

[34] So S-S and Karplus M. (1997). Three-dimensional quantitative structure activity relationships from molecular similarity matrices and genetic neural networks.1. Method and validations. Journal of Medicinal Chemistry, 40, 4347-4359.

[35] Prabhakar YS, Solomon VR, Rawal RK, Gupta MK and Katti SB. (2004). CP-MLR/PLS directed structure–activity modeling of the HIV-1 RT inhibitory activity of 2,3-diaryl-1,3-thiazolidin-4-ones. QSAR and Combinatorial Science, 23, 234-244.

[36] Gramatica P. (2007). Principles of QSAR models validation: internal and external. QSAR and Combinatorial Science, 26, 694-701.

[37] Eriksson L, Jaworska J, Worth AP, Cronin MTD, McDowell RM and Gramatica P.(2003). Methods for reliability and uncertainty assessment and for applicability evaluations of classification and regression-based QSARs. Environmental and Health Perspectives, 111, 1361-1375.

How to cite this article

Parihar R and Sharma BK. (2020). QSAR rationales for the PPARα/γ agonistic activity of 4,4-Dimethyl-1,2,3,4-tetrahydroquinoline derivatives. World Journal of Biology Pharmacy and Health Sciences, 3(1), 38-53.